BBA - Molecular Basis of Disease 1871 (2025) 167699

Contents lists available at ScienceDirect

BBA - Molecular Basis of Disease

journal homepage: www.elsevier.com/locate/bbadis

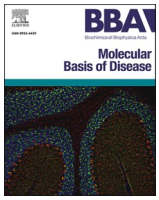

# Amylin is incorporated into extracellular vesicles in an ESCRT-dependent manner and regulates senescence

S. Iglesias-Fortes [a], A.C. Lockwood [a,b,c], C. González-Blanco [a,b,c], D. Lozano [e,f,g], A. García-Aguilar [b,c,d], O. Palomino [b,c,d], G. García [b,c], E. Fernández-Millán [a,b], M. Benito [a], C. Guillén [a,b,c,*]

[a] Department of Biochemistry and Molecular Biology, Faculty of Pharmacy, Complutense University of Madrid, Plaza Ramón y Cajal s/n, Ciudad Universitaria, 28040 Madrid, Spain
[b] CIBER de Diabetes y Enfermedades Metabólicas Asociadas, Instituto de Salud Carlos III, 28040 Madrid, Spain
[c] Department of Biochemistry and Molecular Biology, Faculty of Pharmacy, Complutense University of Madrid, IdISSC, Madrid, Spain
[d] Department of Pharmacology, Pharmacognosy and Botany, Faculty of Pharmacy, Complutense University of Madrid, Madrid, Spain
[e] Instituto de Investigación I+12, Madrid, Spain
[f] Departamento de Química en Ciencias Farmacéuticas, Universidad Complutense de Madrid, Spain
[g] Centro de Investigación Biomédica en Red de Bioingeniería, Biomateriales y Nanomedicina (CIBER-BBN), Instituto de Salud Carlos III, Spain

ARTICLE INFO

*Keywords:*
Amylin
Extracellular vesicles
ESCRT
Senescence
Aggregates
Pancreatic β cells

ABSTRACT

Type 2 diabetes mellitus is a disease which initiates with insulin resistance. Then, pancreatic β cells start to counteract this situation by increasing insulin secretion, which is known as pre-diabetic state. Amylin protein or islet amyloid polypeptide (IAPP), has multiple physiological roles such as the regulation of satiety and avoiding gastric emptying. However, amylin is able to aggregate, forming insoluble structures that affects pancreatic β cell survival. Interestingly, not all the amylin from the different species has this aggregate-prone capacity. There are species, which possesses non-amyloidogenic capacity and does not aggregate such as the rodents. However, there are versions of the protein, for instance from humans and primates, which can aggregate. Previously, we observed that small oligomers could be found in extracellular vesicles (EVs). Now, we have used a pancreatic β cell which overexpresses human amylin (hIAPP) (INS1E-hIAPP) and we have explored the capacity of amylin to be incorporated into EVs and how amylin could affect to different essential signaling pathways such as the mammalian target of rapamycin complex 1, endoplasmic-reticulum stress and senescence. Here, we report that amylin can be incorporated into EVs in an endosomal sorting complexes required for transport (ESCRT)-dependent manner. When we treated the cells with the neutral sphingomyelinase inhibitor, GW4869, one of the pathways for EV biogenesis and under high glucose conditions, there was an increased incorporation of soluble amylin into vesicles. Interestingly in this condition, when we isolated the EVs, we clearly observed that the size of the vesicles was higher, compatible with microvesicles (MVs). Resveratrol increased a pro-senescent phenotype but, it was able to revert either the high glucose or GW4869-associated senescent. In summary, these results indicate that amylin can be recruited in an ESCRT-dependent manner into EVs and, resveratrol presents an important role in inducing senescence in INS1E-hIAPP pancreatic β cells.

## 1. Introduction

Type 2 Diabetes Mellitus (T2DM) is a progressive disease, which is characterized by the existence of an insulin resistance with an increased in pancreatic β cell mass, mainly controlled by the mammalian target of rapamycin complex 1 (mTORC1) signaling pathway [1,2]. This first phase of the disease is the expansive one and it is associated with a hyperinsulinemia and can persist for years. Then, pancreatic β cells start to die by apoptosis [3]. There are alternative situations that lead to apoptosis including a dedifferentiation process from β cells to α cells and an impairment of pancreatic β cells in insulin secretion [4,5]. Amylin is a protein co-secreted with insulin by the β cells controlling a great variety

* Corresponding author at: Department of Biochemistry and Molecular Biology, Faculty of Pharmacy, Complutense University of Madrid, Plaza Ramón y Cajal s/n, Ciudad Universitaria, 28040 Madrid, Spain.
*E-mail address:* cguillen@ucm.es (C. Guillén).

https://doi.org/10.1016/j.bbadis.2025.167699
Received 5 May 2024; Received in revised form 10 January 2025; Accepted 23 January 2025
Available online 30 January 2025

of functions in the organism in the periphery and at the central nervous system including the inhibition of gastric emptying and controlling satiety [6]. However, it can present an intrinsic capacity to aggregate, depending on the type of amylin. There are species that generates a non-amyloidogenic form of the protein, including rodents, and presents in a specific region of the polypeptide several prolines' residues, that impedes β-sheet formation and hence, its aggregation. However, there are another variant of the amylin, which is found in humans and primates, that lacks these prolines and presents a tendency to aggregate and accumulate, contributing to the progressive pancreatic β cell dysfunction in type 2 diabetics [7–11].

As it was previously mentioned, mTORC1 overactivation occurs throughout the progression of the disease. mTORC1 is essential in the control of pancreatic β cell mass but it negatively controls autophagy, which is a protective mechanism in pancreatic β cells [12–18]. Then, under a maintenance of mTORC1 signaling pathway, there is a chronic inactivation of this protective mechanism, leading to dysfunctional pancreatic β cells that accumulates damaged organelles and protein aggregates, that are not correctly eliminated. In fact, we have observed that in a mouse model with a chronic activation of mTORC1 in β cells, there is an accumulation of damaged mitochondria that contributes to the disruption of the cells [19,20]. In addition, we have described that in pancreatic β cells that overexpresses human amylin (hIAPP), a hyperactivation of mTORC1 signaling pathway occurs and an alteration in autophagy and mitophagy processes [21]. Very importantly and as consequence of the disruption of the degradation, an increase in the secretory machinery occurs, generating extracellular vesicles (EVs) bearing small oligomers of amylin. These EVs are secreted and can contribute to the alteration of other cells, permitting the deposition of the toxic protein in other locations [22].

Here, we report that amylin is recognized by the ESCRT machinery for its inclusion into the EVs for its secretion. Interestingly, we have uncovered that under a situation of inhibition of the neutral sphingomyelinase (nSMase) pathway, there is an increased production of bigger structures, which are compatible with microvesicles (MVs) that contains hIAPP, contributing as well to the expansion of the toxic protein. In addition, resveratrol, a polyphenol with multiple protective effects in relation with the induction of autophagy and another actions, induces senescence of the cells and possibly contributes for its elimination by its recognition by immune system.

## 2. Material and methods

### 2.1. Cell lines

Rat insulinoma INS-1E cells were kindly provided by P. Maechler (Université de Genève), and cultured as previously described [23]. Rat insulinoma cell line overexpressing human amylin (INS1E-hIAPP) or overexpressing rat amylin (INS1E-rIAPP) were generously supplied by Anna Novials (IDIBAPS, Barcelona, Spain) and was cultured in 10 % FBS RPMI 1640 medium supplemented with 1 mM sodium pyruvate, 10 mM HEPES, penicillin G (12 μg/mL), streptomycin (10 μg/mL), amphotericin B (0.25 μg/mL), antibiotic-antimycotic 1× and geneticin (G418) (200 μg/mL).

### 2.2. Mice model

Transgenic mice expressing human amylin (hIAPP) under the rat insulin II promoter were developed as FVB/N hemizygous models by the Jackson Laboratory. To obtain heterozygous mice, FVB/N hemizygous transgenic mice were crossed with wild-type (Wt) C57BL/6 mice. Both Tg and Wt mice were subjected to either a standard (STD) diet or a high-fat diet (HFD) for a duration of 8 months, this model was previously described [24].

### 2.3. Antibodies and reagents

The following primary antibodies were obtained from Cell Signalling Technology (Beverly, MA): anti-p70 S6 kinase (#9202), anti-phospho-p70 S6 kinase Thr389 102D2 (#9234), anti-tuberin/TSC2 D93F12 XP (#4308), anti-PERK C33E10 (#3192), anti-phospho-PERK Thr980 16F8 (#3179), anti-BIP C50B12 (#3177), anti-eif2α D7D3, anti-phospho-eif2α Ser51 D9G8 XP (#3398), anti-phospho-histone H2AX Ser139 (#2577), anti-CD81 D502Q (#10037), anti-GM130 D6B1 XP and anti-HRS D7T5N (#15087). Anti DDIT3/GADD153/CHOP sc-7351, p21 (C-19) sc-397, p27 (C-19) sc-528 and anti-TSG101 (C-2) sc-7964 were obtained from Santa Cruz Biotechnology (Dallas, TE). Anti-SIRT-1 (Sir2) was obtained from MERCK Millipore (Burlington, MA). Anti-amylin ab55411 was obtained from Abcam (Cambridge, UK), anti-amylin NBP1–06579 was purchased from Novus Biologicals (Centennial, CO) and anti-β-actin (A2228-200UL) and anti-α-tubulin (T5168-2ML) were obtained from Sigma-Aldrich (St. Louis, MO). Secondary antibodies HRP-conjugated anti-Rabbit (NA934) and anti-Mouse (NA931) were obtained from GE Lifesciences (Marlborough, MA). GW4869 (D1692) was obtained from Sigma-Aldrich (St. Louis, MO). Geneticin (G418) was from Santa Cruz Biotechnology (Dallas, TE). MG5 is an organic compound, generously supplied by Dr. José Carlos Menéndez (School of Pharmacy, UCM, Madrid) used to detect beta sheet like aggregates by immunofluorescence [26]. For IF secondary antibody Donkey anti-Rabbit IgG Alexa Fluor 594 (#A-21207) and Goat anti-Rabbit IgG Alexa Fluor 647 (#A32733) was obtained from Invitrogen. Resveratrol (R5010) was from Sigma-Aldrich (St. Louis, MO).

### 2.4. Treatments

INS-1E hIAPP cells were cultured on a plate with medium changes every 48 h. At 80 % confluence, the medium was changed to 10 % FBS RPMI 1640 enriched in glucose (16,7 mM) and GW4869 20 μM was added, during 24 h. Treatment with resveratrol, dissolved in ethanol to a final concentration of 30 μM, was added during the last 4 h of the experiment.

### 2.5. Western blotting

After the different treatments, cells were washed with PBS 1× and lysed for protein extraction. Protein concentration was determined by the Bradford dye method, using the Bio-Rad® (Hercules, CA) reagent and BSA as standard. Equal amounts of protein (10 μg) were submitted to electrophoresis and after SDS-PAGE gels were transferred to Immobilon PVDF membranes (Merck Millipore, Burlington, MA). Then, membranes were blocked with 5 % BSA and incubated overnight with primary antibodies at 4 °C. The corresponding bands were visualized using the ECL Western blotting protocol (GE Healthcare, Little Chalfont, UK). For the analysis of EVs, lysis buffer was added to part of the exosome suspension for protein extraction according to standard procedures. Electrophoresis was carried out with equal amounts of protein (3–5 μg) and SDS-PAGE gels were transferred to PVDF membranes following the Western Blot wet transfer protocol. After blockade, incubation with primary and secondary antibodies, bands were observed using ECL Western blotting protocol (GE Healthcare, Little Chalfont, UK).

### 2.6. Immunofluorescence

Cells were cultured in glass coverslips to 50 % confluence and fixed using paraformaldehyde 4 % solution during 20 min, permeabilized in PBS with 0,5 % Triton X-100 for 15 min, and then blocked with 3 % BSA, 0,1 % Tween 20 in PBS during 30 min. Cells were incubated overnight at 4 °C with primary antibodies (Amylin 1:100, HRS 1:400; CD81 1:300; TSG101 1:100 in blocking solution) and the corresponding secondary antibody at a dilution of 1:500 for 1 h 30 min. For MG5 imaging, the

compound was diluted in DMSO to 10 μM and cells were incubated with the solution for 30 min before DAPI staining. For quantification, 2 different images were analysed for each experiment and the mean intensity of each region was determined. For analysing the number of aggregates per cell, we used at least 70 cells per condition. After determining a threshold, we analysed the number of elements, and this value was divided by the number of nuclei in the slide, obtaining the mean number of aggregates per cell. For colocalization analysis, the images were processed with Coloc2 choosing different regions of interest (ROI) and the threshold was obtained automatically using Coste's automatic threshold, determining the Pearson's correlation coefficient.

### 2.7. Exosome purification

INS-1E hIAPP cells were grown in 10 % exosome-depleted FBS (Exo-FBSTM) RPMI medium. After the stimulation with different treatments, media was collected and centrifuged at 3000 ×*g* during 15 min to discard cellular debris, filtered by a 0.22 μm filter, mixed with Exo-Quick TCTM exosome isolation reagent and incubated at 4 °C overnight. After that, the mixture was centrifuged at 1500 ×*g* for 30 min, obtaining an exosome-precipitate. Isolated exosomes were resuspended in PBS 1×.

### 2.8. Dynamic light scattering (DLS)

Exosome size and number was analysed by DLS by measuring the rate of Brownian motion of the particles after laser excitation as it was previously performed [22].

### 2.9. β-Galactosidase staining

This procedure was carried out using the cell signaling β-galactosidase staining kit (9860). INS1E-hIAPP cells were grown in 35 mm plates at a density of 30.000 cells/cm$^2$ in 10 % FBS RPMI 1640 medium. After the addition of different treatments, cells were washed with PBS 1× and fixed with 1 mL of fixative solution during 15 min at room temperature (RT). Then, plates were wash 2 times with PBS 1× and 1 mL of the β-galactosidase Staining solution was added and incubated at 37 °C for 48 h in a dry incubator.

### 2.10. Soluble β-galactosidase assay

The procedure was conducted in accordance with the protocol outlined before. Briefly, equal number of cells were seeded and after the treatments, pellets were collected and resuspended in a 0.1 M citrate buffer (pH 4.5). Cellular lysis was achieved through 6 cycles of freezing and thawing, after which the lysates were centrifuged at 11,000 ×*g* for 7 min. The resulting supernatant was then combined with an 2-nitrophenyl-β-D-galactopyranoside (ONPG) solution (2.2 μg/μL) and 1 mM magnesium chloride. The mixture was incubated at 37 °C for 12 h. Finally, absorbance measurements were recorded at 420 nm [25].

### 2.11. IAPP and A11 immunohistochemistry

The first step is a deparaffinization process consisting of a 15-minute xylene run and a battery of alcohols (100 %, 96 %, 90 %, and 70 % ethanol) for 4 min each. Sections were incubated with rabbit polyclonal IAPP antibody (ab55411) and A11 at 1/100 in PBS-Tween/1 % bovine serum antigen overnight at 4 °C. Then, a secondary antibody incubation and development using a diaminobenzidine substrate kit was performed. All images were taken at 20× magnification.

### 2.12. Violet crystal staining

INS1E-hIAPP cells were grown in 12-well plates at a density of 30.000 cells/cm$^2$ in 10 % FBS RPMI 1640 medium. After the different treatments, cells were washed with PBS 1× and stained with 0,2 % violet crystal (w/v) in 2 % ethanol (v/v) for 10 min and gently shaking. Plates were rinsed with ddH2O, dried, and after addition of 1 % sodium dodecyl sulphate (w/v), absorbance at 560 nm was determined for each experimental point.

### 2.13. Proteomic analysis

After treating the sample with 5 volumes of cold acetone (−20 °C) were maintained overnight at −20 °C. The following day, the samples were centrifuged and the supernatant discarded. Afterwards, the pellets were digested for 2 h at 37 °C (iST-Preomics kit). Then, the samples were washed several times and the peptide concentration in the different samples was determined by the Qubit system (Thermo Fisher). Finally, the samples were introduced in the mass spectrophotometer for its analysis. Briefly, the peptides were ionized by electrospray and were analysed in the mass spectrophotometer Q Exactive HF in a DDA (data dependent acquisition) mode. The 10 more intense precursors (charge between +2 and +5) were used for fragmentation HCD (high collision energy dissociation) and the corresponding MSMS spectra were obtained.

### 2.14. Statistical analysis

Statistically significant differences between mean values were determined using either the unpaired Student's *t*-test or ANOVA analysis in the GraphPad statistical analysis software package. Differences were considered statistically significant at $p \leq 0,05$ ($*/^{\#}$ $p \leq 0,05$; $**/^{\#\#}$ $p \leq 0,01$; *** $p \leq 0,005$; n.s. indicates no statistical significance).

## 3. Results

1. Soluble amylin co-localizes with the ESCRT machinery

In a previous paper, we described that amylin aggregates generated by INS1E-hIAPP pancreatic β cells, colocalized with the tumor susceptibility 101 (Tsg101) protein, one of the components of the endosomal sorting complex required for transport (ESCRT)-I machinery [22]. Then, these aggregates could be incorporated into multivesicular bodies during extracellular vesicle biogenesis [27], indicating that amylin aggregates were processed and included into extracellular vesicles (EVs). However, the relevance of ESCRT machinery in hIAPP processing has not been previously described. Firstly, we investigated alterations in extracellular vesicle secretion in response to high glucose concentrations and the inhibition of the n-SMase pathway of EV biogenesis using the inhibitor GW4869. Following the purification of EVs, we conducted dynamic light scattering (DLS) analysis, which revealed an increase in vesicle size upon high glucose (HG) stimulation and a reduction following GW4869 treatment. Notably, a marked increase in EV size was observed with the combined stimulation of high glucose and GW4869 (Fig. 1A). In parallel, we performed Western blot analysis to assess protein content within the EVs. In this analysis, we successfully detected ESCRT-0 vesicle markers, including Tsg101 with CD-63 and Hsp70, alongside the absence of actin, thereby confirming the accuracy of the purification process. Furthermore, we identified the presence of amylin in vesicles derived from INS1E-hIAPP cells (Fig. 1B). Then, we compared EVs obtained from INS1E-hIAPP with two other pancreatic β cell lines, INS1E-WT and INS1E-rIAPP (overexpressing rat amylin, which is not amyloidogenic). Very interestingly, in INS1E-WT and INS1E-rIAPP cells we detected a lower amount or no detection in the interior of EVs, respectively (Fig. 1C and Supplemental Fig. 1). The size distribution of EVs was also determined by DLS in response to the different treatments in both cell lines (Fig. 1D and Supplemental Fig. 1B). We clearly observed a robust colocalization (Pearson's R index of 0,8) of amylin with Hrs, a component of ESCRT-0 machinery, under basal conditions (Fig. 1E). These data suggest that part of the soluble amylin is recognized

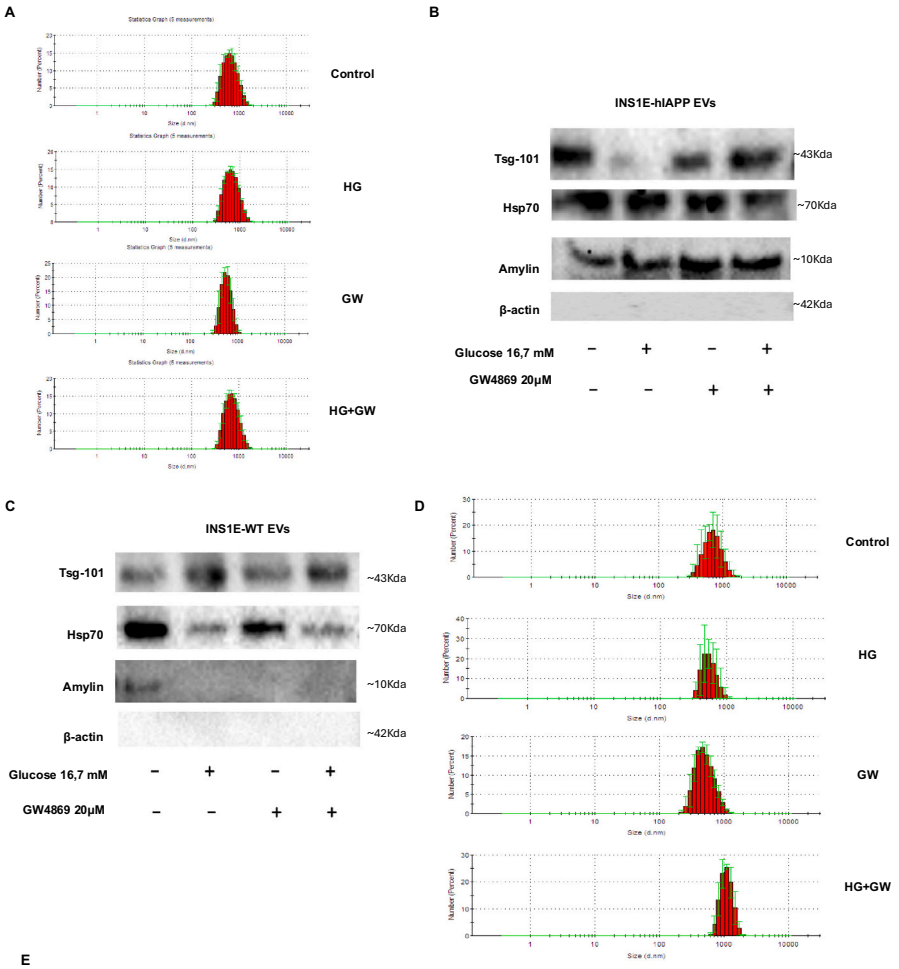


(caption on next page)

**Fig. 1.** Soluble amylin co-localizes with the ESCRT machinery. (A) Extracellular vesicles derived from INS1E-hIAPP cells were analysed for particle size using dynamic light scattering (DLS), and the presence of vesicle markers was assessed *via* Western blotting (B). The same analyses were conducted for extracellular vesicles from INS1E-WT cells (C and D). Immunofluorescence imaging of INS1E-hIAPP cells revealed co-localization of amylin and Hrs (E). In contrast, no co-localization between Tsg101 and amylin was observed in INS1E-WT cells, as shown by immunofluorescence. (F). Amylin levels in INS1E-hIAPP cells were also quantified by Western blot analysis. Data are represented as mean ± SEM, *: $p < 0,05$, ***: $p < 0,001$ ($n = 2–3$). Scale bar, 10 μm.

by the ESCRT-0 system, which is involved in the incorporation of ubiquitinated proteins for EVs biogenesis. In addition, there was an increase in the colocalization signal after the incubation of the cells with either high glucose or blocking the n-SMase EVs biogenesis with the inhibitor GW4869. When we treated the cells with both drugs at the same time, there was a statistically significant increase in the colocalization signal of amylin and Hrs (Fig. 1E).

Then, the fact that amylin is interacting with ESCRT machinery suggested that amylin in INS1E-hIAPP is somehow altered and is being recruited for its elimination by the fusion of MVBs with the lysosomes or for its secretion in the interior of EVs. In order to determine if this interaction between ESCRT machinery and amylin could be detected in INS1E-WT cells, we performed the colocalization analysis between amylin and Tsg101. The data indicated that amylin form INS1E-WT cells did not interact with Tsg101 in any of the treatments (Fig. 1F).

On the other hand, we decided to investigate the effects of high glucose and GW4869 on amylin aggregates in INS1E-hIAPP and INS1E-WT cells. In this context, we observed that high glucose exposure led to an increase in the number of aggregates, although this was not statistically significant. In contrast, treatment with GW4869, either alone or in combination with high glucose, resulted in a statistically significant increase in aggregate accumulation, accompanied by a non-significant increase in the colocalization of Tsg101 and MG5 in INS1E-hIAPP cells (Supplemental Fig. 2). However, in INS1E-WT cells we did not observe any accumulation of aggregates in response to the treatments (Supplemental Fig. 3).

Aggregates could be eliminated by autophagy induction as well [28]. When we pre-treated INS1E-WT and INS1E-hIAPP cells with chloroquine (CQ), which blocks the fusion between autophagosome and lysosome [29], there was an accumulation of aggregates inside the cells, which was reverted by the treatment with resveratrol (Supplemental Fig. 4). When we analysed soluble amylin in these conditions, we corroborated that INS1E-hIAPP presented a basal higher accumulation of amylin compared with INS1E-WT. However, when we added the resveratrol, there was a further increase in soluble amylin in INS1E-hIAPP cells (Supplemental Fig. 5).

2. The reduction of nSMase activity by the use of GW4869 does not alter neither mTORC1 signaling nor ER-stress but, in combination with high glucose, reduces cellular senescence

When we exposed INS1E-hIAPP cells to high glucose, we observed an increase in mTORC1 activity, as indicated by the phosphorylation status of their downstream targets the ribosomal protein S6 and the unc-51 like autophagy activating kinase 1 (ULK1) at serine 757. Simultaneously, there was an elevation in the protein expression ratios of phospho-PERK/PERK and phospho-eIF2α/eIF2α, suggesting the induction of endoplasmic reticulum (ER) stress (Fig. 2A and B). Blocking the formation of extracellular vesicles biogenesis using the GW4869, we did not observe any change neither in the activation of mTORC1 activity nor in the ER-stress. However, when high glucose exposure was combined with GW4869 treatment, we observed a clear tendency toward reducing endoplasmic reticulum stress, marked by a significant decrease in eIF2α phosphorylation (Fig. 2B). This reduction in ER stress was accompanied by the restoration of mTORC1 activity, as indicated by an increased phosphorylation status of S6 and ULK1 at serine 757 (Fig. 2A). Furthermore, when assessing cellular senescence, both high glucose and GW4869 treatments individually promoted a pro-senescent state. Interestingly, the combination of these treatments led to a reduction in the senescent phenotype, evidenced by a reduction in phospho-H2AX protein levels (Fig. 2C) and a decreased in β-galactosidase staining and absorbance (Fig. 2D and F). In addition, any of the treatments affected to cell viability (Fig. 2G).

3. The extracellular vesicles produced by INS1E-hIAPP are enriched in amylin under high glucose conditions and a blockage of nSMase activity

In order to understand the reduction in senescence after the combination of high glucose and the use of GW4869, we studied whether the capacity to secrete EVs could be involved. Firstly, we analysed CD81 accumulation inside the cell by immunofluorescence, as one of the EV's markers, and we determined a reduction in the protein signal after the treatment with either high glucose or the combination of high glucose and GW4869. Remarkably, after the addition of GW4869 under basal glucose conditions there was an accumulation of CD81 protein levels, as expected, although this change was non-statistically significant, indicating that probably there are additional pathways for EVs biogenesis in these cells (Fig. 3A). It is known that resveratrol is a polyphenol which interferes with the aggregation capacity of hIAPP [30]. Since, the combination of high glucose and GW4869 was able to diminish senescence in pancreatic β cells we wanted to analyse if these effects were dependent on the production of enriched-amylin EVs. Then, we purified the EVs obtained from INS1E-hIAPP conditioned-medium (CM) after the exposition under the conditions of the GW4869 with or without resveratrol and the combination of high glucose and GW4869 in the absence or in the presence of resveratrol. We determined by DLS that EVs presented a correct size (Fig. 3B) as well as the identification of a marker found in EVs (Tsg101) as well as the absence of different proteins such as GM130 or β-actin (Fig. 3C). We detected amylin in the interior of the EVs after the combination of high glucose with GW4869 and, more abundantly after the incubation of resveratrol (Fig. 3C). These data indicate that resveratrol is able to facilitate amylin incorporation into the EVs under these conditions, possibly facilitating its accumulation in other locations. Alternatively, we used a comparative proteomic analysis of the EVs for the identification of proteins included in these structures. We found a different composition of proteins depending on the treatment (Supplemental Table 1), and comparing with the top 100 proteins found in the webpage of "Vesiclepedia", we identified from 30 % to 53 % of proteins in all the treatments of our analysis, indicating the correct purification of our EVs (Supplemental Table 2). Very intriguingly, although we did not detect amylin in our proteomic analysis (we detected amylin in the interior of the EVs by western blot analysis in Fig. 3C), we were able to detect amyloid-beta A4 (APP) in the EVs derived from the GW4869 plus resveratrol treatment (Supplemental Table 1, highlighted in brown, line 419). The no identification of amylin in the interior of the EVs from INS1E-hIAPP pancreatic β cells probably was derived from its very small size. Then, we used the GeneCodis tool for analysing the proteins enriched in each treatment by comparing the total proteins detected in the different conditions assessed. We

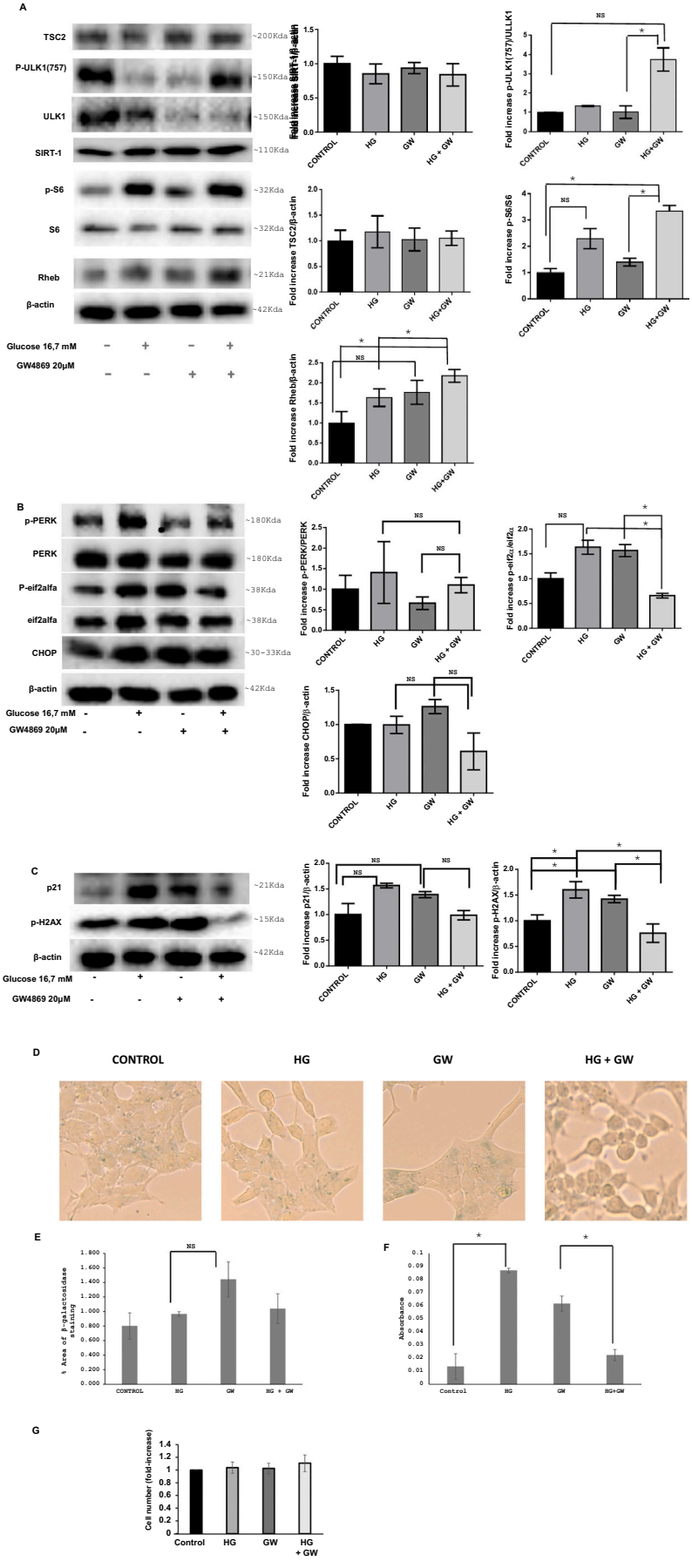


*(caption on next page)*

**Fig. 2.** Analysis of the mTORC1 pathway, ER stress, and senescence in INS1E-hIAPP cells. (A) Proteins associated with the mTORC1 pathway, including phosphorylated S6 (p-S6), phosphorylated ULK1 (Ser757) (p-ULK1), TSC2, SIRT1, and Rheb, were detected by Western blot analysis. (B) Proteins related to ER stress, such as phosphorylated PERK (p-PERK), phosphorylated eIF2α (p-eIF2α), and CHOP, were also assessed by Western blot. (C) Levels of cellular senescence markers p21 and phosphorylated H2AX (p-H2AX) were detected by Western blot. (D,E) β-galactosidase staining performed on INS1E-hIAPP. (F) Absorbance at 420 nm of the procedure performed to measure β-galactosidase activity (pH = 4.5) using ONPG. (G) Cell number quantification. Data are represented as mean ± SEM, *: $p < 0,05$ (n = 2–3).

investigated the two GO categories including biological process (BP) and molecular function (MF), KEGG pathways and reactome significantly different for each treatment [33] (Supplemental Table 3). Curiously, the COPII-coated vesicle cargo loading (line 26 of BP), endoplasmic reticulum to Golgi vesicle-mediated transport (line 36 of BP), positive regulation of extracellular exosome assembly (line 66 of BP), retrograde neuronal dense core vesicle transport (line 96 of BP), synaptic vesicle cycle (line 48 of KEGG pathways) and the vesicle-mediated transport (line 113 of BP and line 456 or reactome) were significantly affected in the EVs produced by INS1E-hIAPP cells under high glucose conditions (HG), resveratrol (RESV) treatment and a blockage of nSMase activity (GW) (Fig. 5).

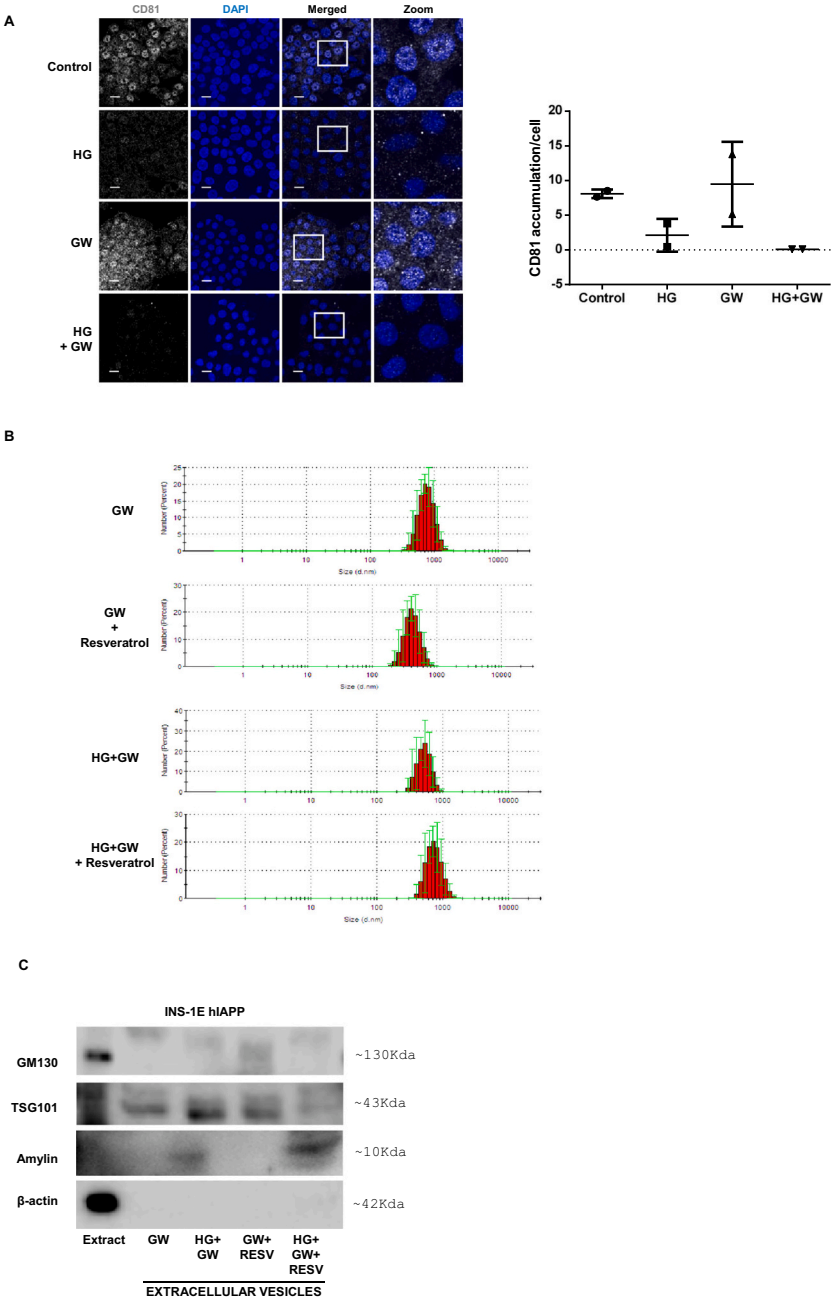


**Fig. 3.** Characterization of extracellular vesicles from INS1E-hIAPP cells treated with resveratrol. (A) Immunofluorescence analysis of INS1E-hIAPP cells showing the detection of CD81, accompanied by its respective quantification. (B) Size distribution of extracellular vesicles isolated from INS1E-hIAPP cells, analysed by DLS. (C) Western blot analysis of extracellular vesicles derived from INS1E-hIAPP cells. The plots indicate mean ± SEM, *: $p < 0,05$ (n = 2–3). Scale bar, 10 μm.

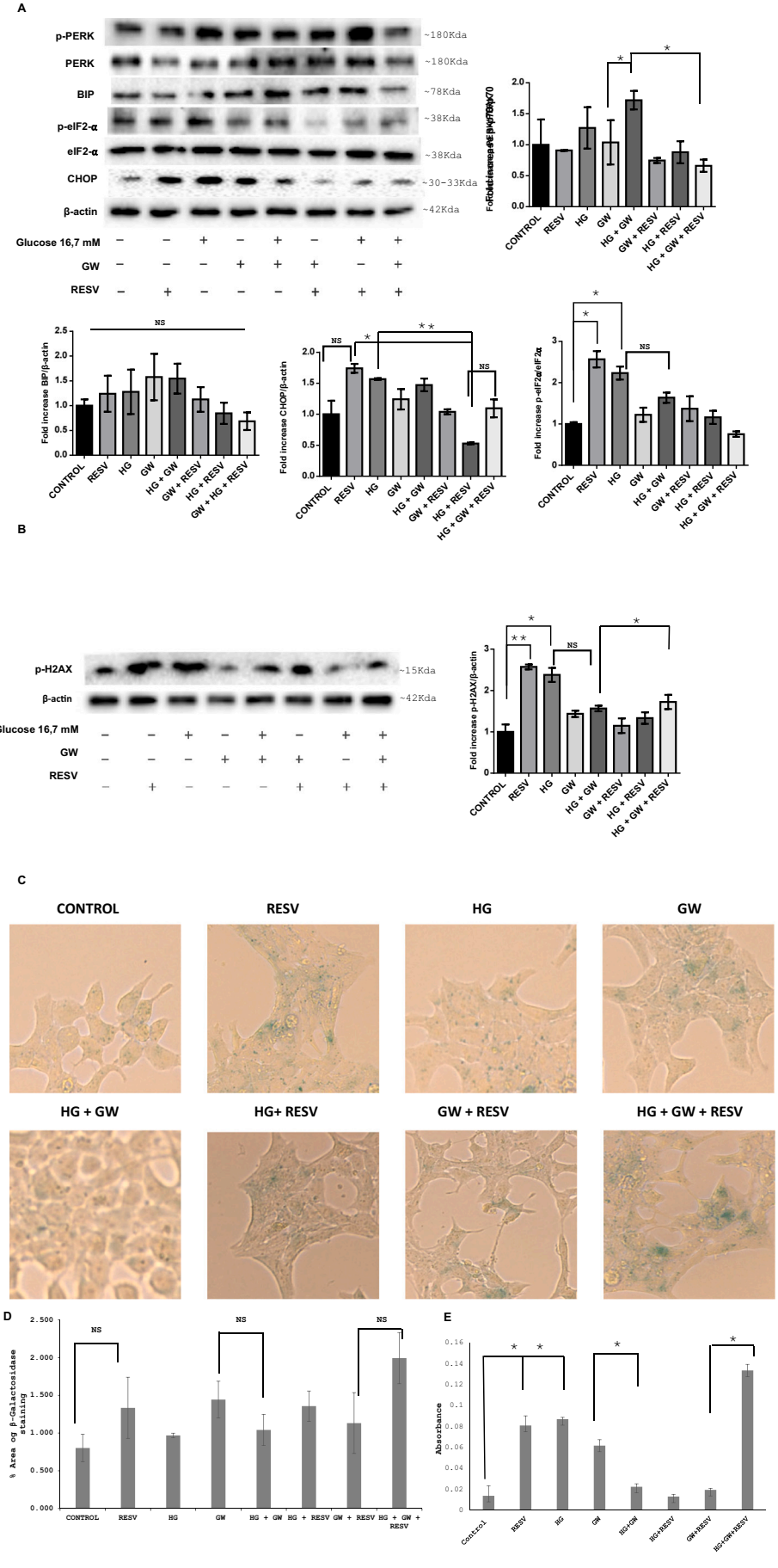


*(caption on next page)*

**Fig. 4.** Effects of resveratrol on INS1E-hIAPP cells treated with GW4869 and high glucose (HG). Western blot analysis of protein levels related to ER stress (A), and p-H2AX (B), in INS1E-hIAPP cells under different treatment conditions. (C, D) β-galactosidase staining was performed in INS1E-hIAPP cells across the different experimental conditions. (E) Absorbance at 420 nm of the procedure performed to measure β-galactosidase activity (pH = 4.5) using ONPG. The plots indicate mean ± SEM, *: $p < 0,05$ **: $p < 0,01$; (n = 2–3).

4. Resveratrol protects from the increased mTORC1 signaling and ER-stress associated with either high glucose, blockage of nSMase activity or its combination but, induces senescence.

When we treated the cells with resveratrol under normal conditions of glucose, there was a reduction in amylin protein levels. A similar result was obtained under high glucose conditions (Supplemental Fig. 6A). This decrease in amylin was associated with a marked reduction in mTORC1 activation (Supplemental Fig. 6B). Although, resveratrol induced an increase in ER-stress (CHOP and phospho-eIF2-α) under normal conditions, there was a decreased phosphorylation status of PERK under high glucose and GW4869 or, in CHOP protein levels under high glucose conditions (Fig. 4A). Very interestingly, when we analysed protein markers such as phospho-H2AX (Fig. 4B) and senescence by β-galactosidase staining (Fig. 4C–D) and absorbance (Fig. 4E), we observed a significantly induction of these parameters in response to resveratrol. Similarly, under high glucose conditions was also observed something similar, which indicates that resveratrol activates a pro-senescence phenotype in these cells. When we treated the cells with GW4869 and under high glucose, resveratrol induced a pro-senescent phenotype as well (Fig. 4B–E).

## 4. Discussion

During the progression to T2DM there is a first phase in which pancreatic β cells increase the proliferative capacity through the upregulation of mTORC1 signaling pathway. However, when this overactivation is maintained generates a chronic ER-stress and an inhibition of autophagy, as a protective mechanism, and makes pancreatic β cells more prone to die by apoptosis [2]. Autophagy is an important mechanism involved in the reduction of the ER-stress and facilitates the elimination of damaged and altered organelles as well as aggregates inside the cells. Using INS1E-hIAPP cells, which overexpresses hIAPP protein levels, we have previously demonstrated alterations in the degradation of mitochondria by mitophagy and an accumulation of polyubiquitinated aggregates associated with an upregulation of mTORC1 pathway [21]. And, more recently, we have uncovered the existence of another mechanism for the elimination of amylin oligomers through the incorporation into extracellular vesicles, exporting these structures outside the cell but facilitating its accumulation in other locations [22].

We observed that amylin aggregates could be recognized by the ESCRT machinery, one of the pathways involved in the generation of intraluminal vesicles (ILV) that will derive to the exosome formation. However, the possible recognition of hIAPP by the ESCRT machinery have never been determined. In this manuscript, we have identified that the Hrs protein, which belongs to the ESCRT-0, involved in the recognition of ubiquitinated cargoes, colocalizes with hIAPP, suggesting that this protein is interacting with one of the initial steps in the EVs biogenesis. In fact, the colocalization signal is very high even under normal glucose conditions, increasing the interaction when we stimulated the cells with high glucose and blocking the nSMase-dependent pathway of EVs biogenesis. In contrast, in INS1-E WT cells, no colocalization with Tsg101 was observed, confirming that the ESCRT machinery specifically recognizes the aggregation-prone and toxic form of amylin. Additionally, western blot analysis revealed a higher concentration of amylin in the vesicles from INS1E-hIAPP cells, with no amylin detected in vesicles from INS1-E WT. Vesicle markers, including Tsg101 and Hsp70, were present, and actin was absent, further confirming the successful purification of the vesicles.

These data suggest that under high glucose conditions, aggregate formation is favored and, in parallel, there is a progressive incorporation of hIAPP into the ESCRT machinery, probably for the generation of EVs. The maximal levels of both parameters were obtained under the

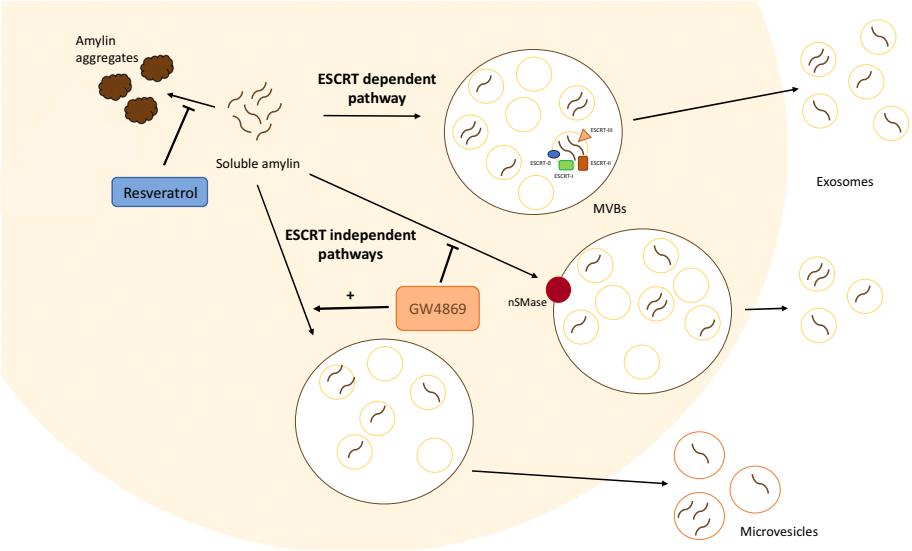


**Fig. 5.** Schematic summary of the work. Amylin interacts with the ESCRT-0 machinery to promote its clearance. Inhibition of the sphingomyelinase-dependent secretory pathway by GW4869 enhances the activation of alternative secretion pathways, facilitating amylin clearance. Additionally, resveratrol, a polyphenol known for its protective properties, induces senescence in these cells, which may promote cell clearance in a physiological context. The mTORC1, ER stress, and senescence pathways were examined under various treatment conditions, including GW4869, high glucose (HG), and their combination, to explore how blocking one secretory pathway—while enhancing an alternative—affects these key cellular processes. The data generated on mTORC1 and ER stress pathways are preliminary, providing a basis for future research.

stimulation with high glucose and the inhibition of the nSMase. Very intriguingly, when we analysed the EVs under the different treatments, we clearly observed that the EV size was higher (300–1000 nm) compared with the size under normal conditions (100 nm) [22], in the absence of GW4869, which could be compatible with the secretion of an alternative type of vesicles, such as MVs. In this regard, it has been noticed in epithelial cells that the addition of GW4869, apart from the inhibition of the nSMase-dependent EV's biogenesis, increased the production of MVs, suggesting that different proteins could be redirected from exosomes to MVs for secretion when the exosome production is partially blocked [34]. Then, when we inhibited the nSMase-dependent formation of EVs, we were able to detect the incorporation of hIAPP into MVs for secretion. In this regard, the propensity of hIAPP to aggregate in pancreatic β cells is one of the factors that influence cellular fate and cell aging [9].

In addition, the administration of GW4869 under high glucose conditions tended to reduce both endoplasmic reticulum stress and cellular senescence, as indicated by β-galactosidase staining and decreased p-H2AX levels. This reduction in ER stress, in turn, reactivated the mTORC1 pathway. Moreover, as previously discussed, the combined treatment increased Hrs colocalization, and we observed elevated levels of amylin in the extracellular vesicles. These findings suggest that inhibiting extracellular vesicle biogenesis through nSMase activity inhibition (*via* GW4869) enhances the incorporation of hIAPP into microvesicles for secretion. Consequently, this process mitigates ER stress, alleviates senescence, and facilitates mTORC1 reactivation.

This mechanism of elimination of a toxic protein into EVs to diminish the toxic effects has been observed in other situations. In fact, in Parkinson's disease, α-synuclein incorporation into EVs have been linked to the propagation of the disease [35]. It has been shown that α-synuclein is incorporated into EVs through the ESCRT machinery and the disruption of this interaction ameliorates the neurodegeneration [36]. In fact, the inhibition of the biogenesis and incorporation of α-synuclein aggregates into EVs, through the inhibition of the nSMase2 activity, reduces the spread of the disease to other locations [37].

Our data suggest that changes in the capacity of β cells to generate amylin in the interior of EVs make susceptible to other tissues to suffer the consequences of the accumulation of this toxic form of the protein. This is very important because it could contribute to understand the potential role of hIAPP to facilitate the appearance of other diabetic complications such as neurodegeneration [22,39–41]. Very importantly, an increased accumulation of hIAPP in the hippocampus accelerates brain aging in a mouse model which overexpresses hIAPP in pancreatic β cells [38]. Intriguingly, in our proteomic analysis, we have identified the amyloid β protein (Aβ) in the interior of the MVs in the condition treated with GW4869, which points to another possible connection between these two pathologies.

In this regard, APP and Aβ have been found in the pancreatic tissue, suggesting that they could play a role in pancreatic function [42]. In addition, the β-site amyloidogenic cleavage of the precursor protein-cleaving enzyme 1 or BACE1, which is a β-secretase involved in the production of Aβ in the brain, have been detected in the pancreas, presenting important functions in pancreatic β cells [43].

These preliminary results reflect that the blockade of one of the secretory pathways involved in the secretion of EVs, can lead to the compensatory activation of alternative secretion pathways, potentially resulting in an increased release of specific proteins that may reach other tissues. This highlights the importance of understanding the relationship of these pathways, as modulating one can influence overall protein trafficking and impact cellular communication.

The role of the polyphenol resveratrol in the inhibition of β-sheet oligomers of hIAPP for blocking its aggregation has been determined [31]. But this inhibition, apart from occurring in hIAPP, can also occur in Aβ [44]. In addition to this effect, resveratrol can disaggregate oligomers, facilitating the appearance of the monomers. These results have been observed in α-synuclein aggregation [45]. However, this effect has not been proven in hIAPP aggregates [45], but the inhibition of amylin aggregation has been clearly demonstrated in response to resveratrol [30,32,46]. Then, resveratrol could potentiate the appearance of higher levels of amylin by its anti-aggregation capacity, inducing ER-stress in the cells. It has been published the capacity of resveratrol to induce ER-stress, growth inhibition and apoptosis in different cell types [47–49]. However, resveratrol protected from ER-stress when INS1E-hIAPP cells were treated with either high glucose (in the case of CHOP protein) or after the treatment with high glucose and GW4869 (for phospho-PERK/PERK ratio). These data indicate that resveratrol, depending on the environment, has different responses. In this regard, the activity of the antioxidants depends on the context [50]. In addition, resveratrol is a potent autophagy inducer and it can facilitate amylin aggregates elimination [21]. In this regard, this protective mechanism could facilitate the maintenance of healthy cells. In addition to this effect, resveratrol induced a senescent phenotype under normal conditions and after the addition of high glucose and GW4869. This pro-senescent and pro-apoptotic effect of resveratrol have been previously described [51,52]. Previous reports from our lab, indicated that resveratrol induced apoptosis in pancreatic β cells [53]. In an *in vivo* context, the promotion of senescent cells is an efficient strategy to limit the progression of damaged cells being correctly removed by the immune system for tissue maintaining under physiological conditions [54,55].

In summary, we have uncovered that hIAPP interacts with the ESCRT machinery, facilitating its incorporation into EVs for its elimination. When we inhibit the nSMase by the use of GW4869, apart from a certain blockade of EV biogenesis and secretion, we permit the formation of alternative sets of MVs that could redirect hIAPP from the EV system to the MV. Then, the appearance of hIAPP in these structures, permits its connection with other pathologies, including neurodegeneration. In addition, we have determined that resveratrol potentiates the induction of senescence, which could potentially facilitate the elimination of these cells by the immune system in a physiological scenario.

Supplementary data to this article can be found online at https://doi.org/10.1016/j.bbadis.2025.167699.

## CRediT authorship contribution statement

**S. Iglesias-Fortes:** Writing – review & editing. **A.C. Lockwood:** Writing – review & editing, Writing – original draft, Methodology, Investigation, Formal analysis. **C. González-Blanco:** Writing – review & editing, Software, Methodology, Investigation, Formal analysis. **D. Lozano:** Investigation. **A. García-Aguilar:** Writing – review & editing, Writing – original draft, Software, Investigation, Formal analysis. **O. Palomino:** Writing – review & editing. **G. García:** Writing – review & editing. **M. Benito:** Supervision, Funding acquisition. **C. Guillén:** Writing – review & editing, Writing – original draft, Validation, Supervision, Software, Project administration, Funding acquisition, Conceptualization.

## Declaration of competing interest

The authors declare that they have no known competing financial interests or personal relationships that could have appeared to influence the work reported in this paper.

## Acknowledgements

This work was funded by the Ministerio de Ciencia e Innovación (PID2020-113361RB-I00). We thank to P2022/BMD-7227, MOIR-ACTOME-CM. Dirección General de Investigación e Innovación Tecnológica (DGIIT), Consejería de Educación y Universidades. Comunidad de Madrid, Madrid, España. We would like to thank Elena González for her assistance in the laboratory. The proteomic analysis was performed in the Proteomics Unit (CAI Biological Techniques) of Complutense University of Madrid.

## Data availability

The datasets used during the current study are available from the corresponding author on reasonable request.

## References

[1] A. Bartolome, C. Guillen, Role of the mammalian target of rapamycin (mTOR) complexes in pancreatic beta-cell mass regulation, Vitam. Horm. 95 (2014) 425–469.
[2] C. Guillen, M. Benito, mTORC1 overactivation as a key aging factor in the progression to type 2 diabetes mellitus, Front. Endocrinol. (Lausanne) 9 (2018) 621.
[3] K. Maedler, Beta cells in type 2 diabetes - a crucial contribution to pathogenesis, Diabetes Obes. Metab. 10 (2008) 408–420.
[4] C. Talchai, H.V. Lin, T. Kitamura, D. Accili, Genetic and biochemical pathways of beta-cell failure in type 2 diabetes, Diabetes Obes. Metab. 11 (Suppl. 4) (2009) 38–45.
[5] D. Accili, S.C. Talchai, J.Y. Kim-Muller, F. Cinti, E. Ishida, A.M. Ordelheide, T. Kuo, J. Fan, J. Son, When beta-cells fail: lessons from dedifferentiation, Diabetes Obes. Metab. 18 (Suppl. 1) (2016) 117–122.
[6] T.A. Lutz, Creating the amylin story, Appetite 172 (2022) 105965.
[7] S. Hassan, K. White, C. Terry, Linking hIAPP misfolding and aggregation with type 2 diabetes mellitus: a structural perspective, Biosci. Rep. 42 (2022) BSR20211297.
[8] A.F. Raimundo, S. Ferreira, I.C. Martins, R. Menezes, Islet amyloid polypeptide: a partner in crime with abeta in the pathology of Alzheimer's disease, Front. Mol. Neurosci. 13 (2020) 35.
[9] M. Press, T. Jung, J. Konig, T. Grune, A. Hohn, Protein aggregates and proteostasis in aging: amylin and beta-cell function, Mech. Ageing Dev. 177 (2019) 46–54.
[10] R. Akter, P. Cao, H. Noor, Z. Ridgway, L.H. Tu, H. Wang, A.G. Wong, X. Zhang, A. Abedini, A.M. Schmidt, D.P. Raleigh, Islet amyloid polypeptide: structure, function, and pathophysiology, J. Diabetes Res. 2016 (2016) 2798269.
[11] P. Westermark, A. Andersson, G.T. Westermark, Islet amyloid polypeptide, islet amyloid, and diabetes mellitus, Physiol. Rev. 91 (2011) 795–826.
[12] M. Bugliani, S. Mossuto, F. Grano, M. Suleiman, L. Marselli, U. Boggi, P. De Simone, D.L. Eizirik, M. Cnop, P. Marchetti, V. De Tata, Modulation of autophagy influences the function and survival of human pancreatic beta cells under endoplasmic reticulum stress conditions and in type 2 diabetes, Front. Endocrinol. (Lausanne) 10 (2019) 52.
[13] Q. Sheng, X. Xiao, K. Prasadan, C. Chen, Y. Ming, J. Fusco, N.N. Gangopadhyay, D. Ricks, G.K. Gittes, Autophagy protects pancreatic beta cell mass and function in the setting of a high-fat and high-glucose diet, Sci. Rep. 7 (2017) 16348.
[14] P. Marchetti, M. Masini, Autophagy and the pancreatic beta-cell in human type 2 diabetes, Autophagy 5 (2009) 1055–1056.
[15] Y. Fujitani, C. Ebato, T. Uchida, R. Kawamori, H. Watada, Beta-cell autophagy: a novel mechanism regulating beta-cell function and mass: lessons from beta-cell-specific Atg7-deficient mice, Islets 1 (2009) 151–153.
[16] Y. Fujitani, R. Kawamori, H. Watada, The role of autophagy in pancreatic beta-cell and diabetes, Autophagy 5 (2009) 280–282.
[17] C. Ebato, T. Uchida, M. Arakawa, M. Komatsu, T. Ueno, K. Komiya, K. Azuma, T. Hirose, K. Tanaka, E. Kominami, R. Kawamori, Y. Fujitani, H. Watada, Autophagy is important in islet homeostasis and compensatory increase of beta cell mass in response to high-fat diet, Cell Metab. 8 (2008) 325–332.
[18] H.S. Jung, K.W. Chung, J. Won Kim, J. Kim, M. Komatsu, K. Tanaka, Y.H. Nguyen, T.M. Kang, K.H. Yoon, J.W. Kim, Y.T. Jeong, M.S. Han, M.K. Lee, K.W. Kim, J. Shin, M.S. Lee, Loss of autophagy diminishes pancreatic beta cell mass and function with resultant hyperglycemia, Cell Metab. 8 (2008) 318–324.
[19] A. Bartolome, M. Kimura-Koyanagi, S. Asahara, C. Guillen, H. Inoue, K. Teruyama, S. Shimizu, A. Kanno, A. Garcia-Aguilar, M. Koike, Y. Uchiyama, M. Benito, T. Noda, Y. Kido, Pancreatic beta-cell failure mediated by mTORC1 hyperactivity and autophagic impairment, Diabetes 63 (2014) 2996–3008.
[20] A. Bartolome, A. Garcia-Aguilar, S.I. Asahara, Y. Kido, C. Guillen, U.B. Pajvani, M. Benito, MTORC1 regulates both general autophagy and mitophagy induction after oxidative phosphorylation uncoupling, Mol. Cell. Biol. 37 (2017) (e00441-17).
[21] M.G. Hernandez, A.G. Aguilar, J. Burillo, R.G. Oca, M.A. Manca, A. Novials, G. Alcarraz-Vizan, C. Guillen, M. Benito, Pancreatic beta cells overexpressing hIAPP impaired mitophagy and unbalanced mitochondrial dynamics, Cell Death Dis. 9 (2018) 481.
[22] J. Burillo, M. Fernandez-Rhodes, M. Piquero, P. Lopez-Alvarado, J.C. Menendez, B. Jimenez, C. Gonzalez-Blanco, P. Marques, C. Guillen, M. Benito, Human amylin aggregates release within exosomes as a protective mechanism in pancreatic beta cells: pancreatic beta-hippocampal cell communication, Biochim. Biophys. Acta, Mol. Cell Res. 1868 (2021) 118971.
[23] A. Merglen, S. Theander, B. Rubi, G. Chaffard, C.B. Wollheim, P. Maechler, Glucose sensitivity and metabolism-secretion coupling studied during two-year continuous culture in INS-1E insulinoma cells, Endocrinology 145 (2004) 667–678.
[24] S. Iglesias-Fortes, C. González-Blanco, A. García-Carrasco, A. Izquierdo-Lahuerta, G. García, A. García-Aguilar, A. Lockwood, O. Palomino, G. Medina-Gómez, M. Benito, C. Guillén, The overexpression of human amylin in pancreatic β cells facilitate the appearance of amylin aggregates in the kidney contributing to diabetic nephropathy, Sci. Rep. 14 (1) (2024 Oct 21) 24729, https://doi.org/10.1038/s41598-024-77063-9 (PMID: 39433955; PMCID: PMC11494195).
[25] B.Y. Lee, J.A. Han, J.S. Im, A. Morrone, K. Johung, E.C. Goodwin, W.J. Kleijer, D. DiMaio, E.S. Hwang, Senescence-associated beta-galactosidase is lysosomal beta-galactosidase, Aging Cell 5 (2) (2006 Apr) 187–195, https://doi.org/10.1111/j.1474-9726.2006.00199.x (PMID: 16626397).
[26] M. Staderini, S. Aulic, M. Bartolini, H.N. Tran, V. Gonzalez-Ruiz, D.I. Perez, N. Cabezas, A. Martinez, M.A. Martin, V. Andrisano, G. Legname, J.C. Menendez, M.L. Bolognesi, A fluorescent styrylquinoline with combined therapeutic and diagnostic activities against Alzheimer's and prion diseases, ACS Med. Chem. Lett. 4 (2013) 225–229.
[27] M. Colombo, G. Raposo, C. Thery, Biogenesis, secretion, and intercellular interactions of exosomes and other extracellular vesicles, Annu. Rev. Cell Dev. Biol. 30 (2014) 255–289.
[28] B. Bauer, S. Martens, L. Ferrari, Aggrephagy at a glance, J. Cell Sci. 136 (2023) jcs260888.
[29] M. Mauthe, I. Orhon, C. Rocchi, X. Zhou, M. Luhr, K.J. Hijlkema, R.P. Coppes, N. Engedal, M. Mari, F. Reggiori, Chloroquine inhibits autophagic flux by decreasing autophagosome-lysosome fusion, Autophagy 14 (2018) 1435–1455.
[30] F. Lolicato, A. Raudino, D. Milardi, C. La Rosa, Resveratrol interferes with the aggregation of membrane-bound human-IAPP: a molecular dynamics study, Eur. J. Med. Chem. 92 (2015) 876–881.
[31] P. Jiang, W. Li, J.E. Shea, Y. Mu, Resveratrol inhibits the formation of multiple-layered beta-sheet oligomers of the human islet amyloid polypeptide segment 22-27, Biophys. J. 100 (2011) 1550–1558.
[32] A. Pithadia, J.R. Brender, C.A. Fierke, A. Ramamoorthy, Inhibition of IAPP aggregation and toxicity by natural products and derivatives, J. Diabetes Res. 2016 (2016) 2046327.
[33] A. Garcia-Moreno, R. Lopez-Dominguez, J.A. Villatoro-Garcia, A. Ramirez-Mena, E. Aparicio-Puerta, M. Hackenberg, A. Pascual-Montano, P. Carmona-Saez, Functional enrichment analysis of regulatory elements, Biomedicines 10 (2022).
[34] K. Menck, C. Sonmezer, T.S. Worst, M. Schulz, G.H. Dihazi, F. Streit, G. Erdmann, S. Kling, M. Boutros, C. Binder, J.C. Gross, Neutral sphingomyelinases control extracellular vesicles budding from the plasma membrane, J. Extracell. Vesicles 6 (2017) 1378056.
[35] L.E. Shippey, S.G. Campbell, A.F. Hill, D.P. Smith, Propagation of Parkinson's disease by extracellular vesicle production and secretion, Biochem. Soc. Trans. 50 (2022) 1303–1314.
[36] S. Nim, D.M. O'Hara, C. Corbi-Verge, A. Perez-Riba, K. Fujisawa, M. Kapadia, H. Chau, F. Albanese, G. Pawar, M.L. De Snoo, S.G. Ngana, J. Kim, O.M.A. El-Agnaf, E. Rennella, L.E. Kay, S.K. Kalia, L.V. Kalia, P.M. Kim, Disrupting the alpha-synuclein-ESCRT interaction with a peptide inhibitor mitigates neurodegeneration in preclinical models of Parkinson's disease, Nat. Commun. 14 (2023) 2150.
[37] V. Sackmann, M.S. Sinha, C. Sackmann, L. Civitelli, J. Bergstrom, A. Ansell-Schultz, M. Hallbeck, Inhibition of nSMase2 reduces the transfer of oligomeric alpha-synuclein irrespective of hypoxia, Front. Mol. Neurosci. 12 (2019) 200.
[38] X. Dong, J. Nao, J. Shi, D. Zheng, Predictive value of routine peripheral blood biomarkers in Alzheimer's disease, Front. Aging Neurosci. 11 (2019) 332.
[39] M. Alrouji, H.M. Al-Kuraishy, A.I. Al-Gareeb, A. Alexiou, M. Papadakis, H.M. Saad, G.E. Batiha, The potential role of human islet amyloid polypeptide in type 2 diabetes mellitus and Alzheimer's diseases, Diabetol. Metab. Syndr. 15 (2023) 101.
[40] T.A. Lutz, U. Meyer, Amylin at the interface between metabolic and neurodegenerative disorders, Front. Neurosci. 9 (2015) 216.
[41] I. Martinez-Valbuena, R. Valenti-Azcarate, I. Amat-Villegas, M. Riverol, I. Marcilla, C.E. de Andrea, J.A. Sanchez-Arias, M. Del Mar Carmona-Abellan, G. Marti, M. E. Erro, E. Martinez-Vila, M.T. Tunon, M.R. Luquin, Amylin as a potential link between type 2 diabetes and Alzheimer disease, Ann. Neurol. 86 (2019) 539–551.
[42] J.A. Kulas, K.L. Puig, C.K. Combs, Amyloid precursor protein in pancreatic islets, J. Endocrinol. 235 (2017) 49–67.
[43] S. Casas, P. Casini, S. Piquer, J. Altirriba, M. Soty, L. Cadavez, R. Gomis, A. Novials, BACE2 plays a role in the insulin receptor trafficking in pancreatic ss-cells, Am. J. Physiol. Endocrinol. Metab. 299 (2010) E1087–E1095.
[44] F. Li, C. Zhan, X. Dong, G. Wei, Molecular mechanisms of resveratrol and EGCG in the inhibition of Abeta(42) aggregation and disruption of Abeta(42) protofibril: similarities and differences, Phys. Chem. Chem. Phys. 23 (2021) 18843–18854.
[45] E. Chau, H. Kim, J. Shin, A. Martinez, J.R. Kim, Inhibition of alpha-synuclein aggregation by AM17, a synthetic resveratrol derivative, Biochem. Biophys. Res. Commun. 574 (2021) 85–90.
[46] P. Nedumpully-Govindan, A. Kakinen, E.H. Pilkington, T.P. Davis, P. Chun Ke, F. Ding, Stabilizing off-pathway oligomers by polyphenol nanoassemblies for IAPP aggregation inhibition, Sci. Rep. 6 (2016) 19463.
[47] J.R. Heo, S.M. Kim, K.A. Hwang, J.H. Kang, K.C. Choi, Resveratrol induced reactive oxygen species and endoplasmic reticulum stress-mediated apoptosis, and cell

cycle arrest in the A375SM malignant melanoma cell line, Int. J. Mol. Med. 42 (2018) 1427–1435.
[48] J.W. Park, W.G. Choi, P.J. Lee, S.W. Chung, B.S. Kim, H.T. Chung, S. Cho, J.H. Kim, B.H. Kang, H. Kim, H.P. Kim, S.H. Back, The novel resveratrol derivative 3,5-diethoxy-3′,4′-dihydroxy-trans-stilbene induces mitochondrial ROS-mediated ER stress and cell death in human hepatoma cells in vitro, Acta Pharmacol. Sin. 38 (2017) 1486–1500.
[49] I. Papandreou, M. Verras, B. McNeil, A.C. Koong, N.C. Denko, Plant stilbenes induce endoplasmic reticulum stress and their anti-cancer activity can be enhanced by inhibitors of autophagy, Exp. Cell Res. 339 (2015) 147–153.
[50] I. Tyuryaeva, O. Lyublinskaya, Expected and unexpected effects of pharmacological antioxidants, Int. J. Mol. Sci. 24 (2023).
[51] L.L. Zamin, E.C. Filippi-Chiela, P. Dillenburg-Pilla, F. Horn, C. Salbego, G. Lenz, Resveratrol and quercetin cooperate to induce senescence-like growth arrest in C6 rat glioma cells, Cancer Sci. 100 (2009) 1655–1662.
[52] H. Luo, A. Yang, B.A. Schulte, M.J. Wargovich, G.Y. Wang, Resveratrol induces premature senescence in lung cancer cells via ROS-mediated DNA damage, PLoS One 8 (2013) e60065.
[53] A. Garcia-Aguilar, C. Guillen, M. Nellist, A. Bartolome, M. Benito, TSC2 N-terminal lysine acetylation status affects to its stability modulating mTORC1 signaling and autophagy, Biochim. Biophys. Acta 2016 (1863) 2658–2667.
[54] D.G.A. Burton, A. Stolzing, Cellular senescence: immunosurveillance and future immunotherapy, Ageing Res. Rev. 43 (2018) 17–25.
[55] B. Li, D. Hou, H. Guo, H. Zhou, S. Zhang, X. Xu, Q. Liu, X. Zhang, Y. Zou, Y. Gong, C. Shao, Resveratrol sequentially induces replication and oxidative stresses to drive p53-CXCR2 mediated cellular senescence in cancer cells, Sci. Rep. 7 (2017) 208.